Phys. Status Solidi B **251,** No. 11, 2189–2192 (2014) / **DOI** 10.1002/pssb.201400028

physica status solidi b
www.pss-b.com
basic solid state physics

DLTS characterization of proton-implanted silicon under varying annealing conditions

J. G. Laven*[,1], M. Jelinek[,2], R. Job[3], W. Schustereder[2], H.-J. Schulze[1], M. Rommel[4], and L. Frey[4,5]**

[1] Infineon Technologies AG, 81726 Munich, Germany
[2] Infineon Technologies Austria AG, 9500 Villach, Austria
[3] Department of Electrical Engineering and Computer Science, Muenster University of Applied Sciences, 48565 Steinfurt, Germany
[4] Fraunhofer Institute for Integrated Systems and Device Technology (IISB), 91058 Erlangen, Germany
[5] Chair of Electron Devices, University of Erlangen-Nuremberg, 91058 Erlangen, Germany

Received 28 April 2014, revised 18 May 2014, accepted 21 May 2014
Published online 10 September 2014

Keywords deep-level defects, hydrogen, proton implantation, silicon

* Corresponding author: e-mail johannes.laven@infineon.com, Phone: +49 89 234 21945, Fax: +49 89 234 152 1945
** e-mail moriz.jelinek@infineon.com, Phone: +43 5 1777 18048

Deep-level defects remaining in the upper half of the band-gap of silicon implanted with protons at fluences and annealing temperatures typically used for proton-implantation doping are investigated. For proton fluences in the range of several $10^{13}\,cm^{-2}$ to several $10^{14}\,cm^{-2}$, a multitude of deep-level defects remain active in comparatively high concentrations of up to $10^{13}\,cm^{-3}$ even after anneals at temperatures up to 500 °C. The detected deep-levels are assigned to known lattice defects on the basis of their electrical characteristics obtained by Fourier-transform DLTS measurements. Despite the low oxygen content of the float-zone silicon used, a large number of the detected defects are ascribed to (non-)hydrogenated vacancy-oxygen defects. The annealing temperature ranges, in which the deep-level defects were detected, are shown. Furthermore, the dependencies of the deep-level defects on the proton fluence and their depth distributions in the implantation profile are investigated.

1 Introduction Proton implantations find wide-spread application in the tailoring of modern power semiconductor devices [1, 2]. The comparatively high penetration range of protons allows a well-controlled modification of the electrical properties of the semiconductor substrate in a spatial range spanning four orders of magnitude between a depth of about 100 nm and 1 mm. The characteristic shape of the induced damage profiles exhibits an extended penetrated range with an approximately constant damage concentration followed by an excess damage peak near the end-of-range of the protons. Thus, using multiple implantations, deep and complex profiles can be designed.

At fluences up to about $1 \times 10^{13}\,cm^{-2}$ and annealing temperatures up to about 200–300 °C, proton implantations are mainly used to reduce the charge-carrier (cc) lifetime in bipolar power devices such as thyristors [3] or diodes [4]. A multitude of electrically active deep-level defects (DL) are known to form in proton-implanted silicon (see, e.g., Refs. [1, 5]). For proton fluences above several $10^{12}\,cm^{-2}$, hydrogen-related donors (HDs) appear [6–8]. These HDs are, in general, undesired in applications aiming to reduce the cc lifetime [9]. On the other hand, HDs may be deliberately used to tailor the doping profiles of power semiconductor devices [10, 11]. The activation of HD profiles requires a thermal budget well above the typical annealing parameters used for cc lifetime reduction [12, 13]. In comparison to conventional doping techniques, HD doping allows control over the doping profile deep in the power semiconductor device at moderate thermal budgets and implantation energies.

Although many studies are concerned with DLs induced by proton implantations, only few investigate the parameter space of high proton doses ($>3 \times 10^{13}\,cm^{-2}$) and elevated annealing temperatures (350–500 °C) typically used for HD doping (see, e.g., Ref. [14]). For power semiconductor devices making use of the HDs, the knowledge of remaining DLs and their impact on the cc lifetime is, however, of considerable interest.

2 Experimental Commercially available <100>-oriented phosphorus-doped float-zone (FZ) silicon wafers with a specific resistivity of 120 Ωcm were used in this study. In

order to remove any crystal originated particles (COPs) remaining in the as-received wafers, the samples were oxidized at elevated temperatures. The resulting oxide film was subsequently removed by wet-chemical etching. On some samples, circular p^+n-diode structures with a radius of 0.75 mm were created by a masked BF_2-implantation (20 keV, $1 \times 10^{14}\,cm^{-2}$, 7° tilt) followed by a thermal annealing step (1050 °C, 1 h, inert) to activate the implanted boron and anneal-out any crystal damage caused by the BF_2-implantation. Shortly after removing any native oxide, the diode structures were metallized by a structured vapor deposition of 100 nm Ti and 400 nm Al. The metal contact structures were centered on the p^+-diode structures and had a smaller radius of 0.5 mm, in order to avoid shortening the diode structures. The prepared wafers were then implanted with protons with an energy of 2.3 MeV and fluences between 3×10^{13} and $4 \times 10^{14}\,cm^{-2}$ through Al absorbers with thicknesses of 35 μm or 50 μm. Following the proton implantation the samples were annealed at temperatures between 350 °C and 500 °C for 5 h. For the depth profile in Fig. 4, the sample was directly implanted with 2.5-MeV protons and metallized by Pd-Schottky contacts after annealing and beveling. The proton-induced DLs were analyzed by Fourier-transform DLTS measurements [15] using a PhysTech FT 1030 measurement and analysis system. During the measurements, the diode structures were reverse-biased between −2 V and −5 V. The measurements were initiated by a 1-ms filling pulse at −1 V.

3 Results and discussion Figure 1 shows selected DLTS spectra recorded in proton-implanted samples after annealing at different temperatures. Reference samples not implanted with protons showed no detectable DLs apart from a very weak signal of DL S (not shown). Hence, all DLs visible in Fig. 1 are induced by the proton implantation and successive annealing. The detected DLs from this and other measurements are summed up in Table 1 together with their characteristics and presumed identifications. DLs which coincide within the error range given in Table 1 are hereby assumed to be identical in different samples.

Table 1 Characteristic parameters of DLs in H^+-implanted FZ Si.

DL	$E_C - E_{DL}$ (meV)	σ_{Arr} ($10^{-15}\,cm^2$)	presumed identification
A	60 ± 8	4 ± 3	$OTDD^{0/+}$ and unknown
B1	104 ± 10	263 ± 284	$OTD^{0/+}$
B2	103 ± 6	32 ± 6	unknown
C1	103 ± 9	1.0 ± 0.7	$C_iO_i\text{-}H^{-/0}$
C2	125 ± 7	10 ± 4	(C-H) ?
C3	130 ± 7	11 ± 3	see C2
D	151 ± 7	5 ± 2	$OTDD^{+/2+}$
E	173 ± 7	6 ± 2	$VO^{-/0}$
F	173 ± 7	0.14 ± 0.02	$V_2O_2{}^{2-/-}$
G	212 ± 7	31 ± 6	$(V_2O^{2-/-})$?
H	226 ± 8	9 ± 3	$V_2{}^{2-/-}$
I	278 ± 7	10 ± 1	unknown
K	300 ± 8	2.1 ± 0.4	$V_2H_2{}^{-/0}$ and $X^{-/0}$
L	333 ± 8	6 ± 2	$VOH^{-/0}$
M1	418 ± 7	14 ± 2	$V_2O_2{}^{-/0}$ and $X^{2-/-}$
M2	437 ± 9	23 ± 5	$V_2H^{-/0}$ and $V_2{}^{-/0}$
P	469 ± 11	5 ± 2	$V_2O^{-/0}$
S	568 ± 10	2.1 ± 0.4	V-rel/N-rel

The detected DLs of Table 1 are mostly attributed to DLs known to originate from lattice damage or hydrogenated crystal defects. Despite the low oxygen content in the used FZ silicon ($\sim 3 \times 10^{15}\,cm^{-3}$), the DLs A, B1, and D are assigned to oxygen-related thermal double-donors (OTDD) [16] or thermal donors (OTD) [17]. Radiation damage as well as hydrogen are known to enhance the generation rate of OTD(D)s [18, 19]. C1 is presumed to be identical to a donor-defect reported in hydrogenated and electron-irradiated oxygen-rich silicon [20]. In sum, the *quasi-shallow* DLs A, B1, and C1 may account for up to 5–10% of the simultaneously induced shallow HDs. Figure 2 depicts the annealing temperature ranges in which the DLs were detected (thick black lines). DL A exists in a temperature range typical for OTDDs. The disappearance of the minor signal of B1 above annealing temperatures of 400 °C may well be due to a superposition by the signal A.

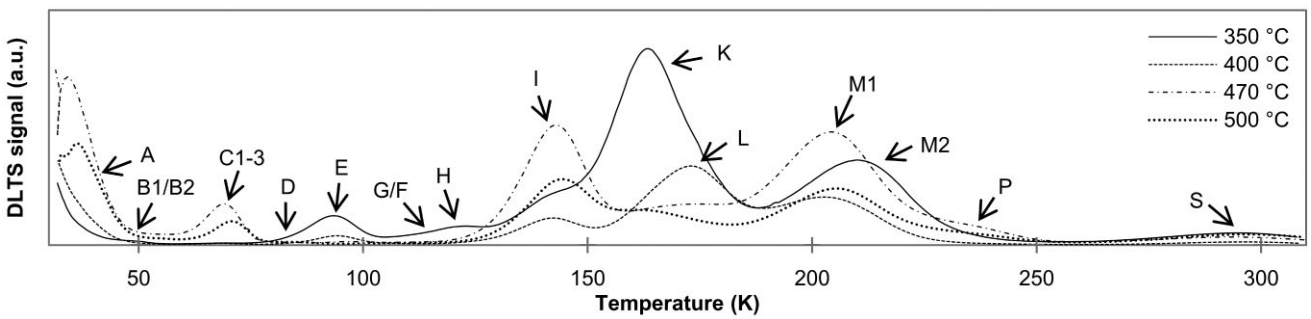

Figure 1 DLTS spectra (48.8 Hz window) in samples implanted with 2.3-MeV protons through a 50 μm (350 °C) or 35 μm (400–500 °C) thick Al-absorber with fluences of $3 \times 10^{13}\,cm^{-2}$ (350 °C) or $4 \times 10^{14}\,cm^{-2}$ (400–500 °C) annealed at 350–500 °C for 5 h.

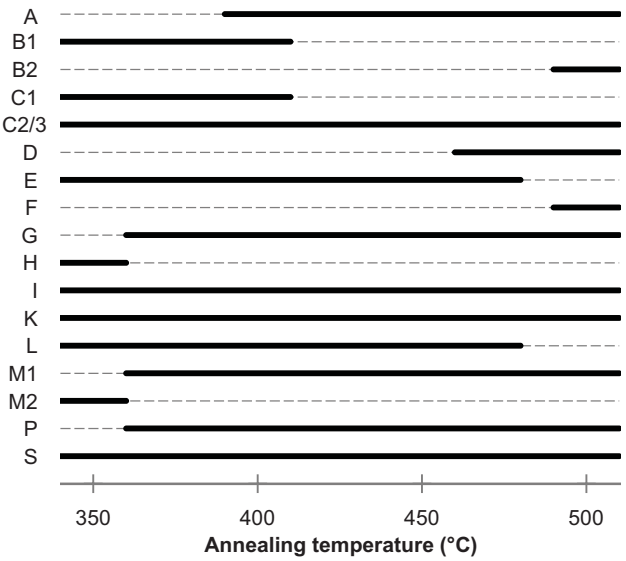

Figure 2 Annealing temperature ranges in which the DLs of Table 1 were detected in high-dose H^+-implanted Si samples. All anneals lasted 5 h.

The electrical properties of the DL E are in good agreement with those of the A-center (VO) (see, e.g., Ref. [21]). Despite its low thermal stability, the A-center has already been reported to exist after thermal anneals above 400 °C for proton implants with a fluence of 1×10^{13} cm^{-3} [22]. The DLs F and G are tentatively ascribed to the second ionization levels of the higher-order vacancy-oxygen defects V_2O_2 and V_2O, respectively. The first ionization levels of these defects are assigned, at least partially, to the signals M1 and P, respectively. The appearance of the DL F coincides with the vanishing of the alleged A-center, DL E. The accumulation of mobile A-centers to V_2O_2-defects is a reasonable reaction path at elevated temperatures beyond the migration barrier of the A-center [23]. The appearance of V_2O is known to correlate with the annealing of the divacancy V_2 [24, 25]. This is in good agreement with the disappearance of the DLs H and M2. In further agreement of the electrical characteristics, the DLs H and M1 are attributed to the second and first ionization levels of the divacancy, respectively [26]. The divacancy is known to be instable already at the lowest annealing temperatures examined in this study. The low signal of DL H is, hence, expected to be only the remainder of a higher concentration of divacancies at lower annealing temperatures. Only a minor part of the signal M1 is ascribed to the first ionization level of the divacancy due to a significant interaction between the signals of the DLs M1 and K in dependence of the filling pulse duration.[1] For the time being, the major portion of the signals M1 and K is assigned to an arbitrary defect X. The other fraction of the signal K is expected to originate from a two-fold hydrogenated divacancy V_2H_2 [27, 28]. The electrical characteristics of the DL L, as well as its thermal correlation with the supposed A-center (DL E) justify its assignment to the hydrogenated A-center VO-H [29]. The signal M2 is partially ascribed to the first ionization level of the divacancy and, for the major percentage, to the singly hydrogenated divacancy V_2H [30]. Both defects have only a low thermal stability and are, hence, fully annealed-out at annealing temperatures above 350 °C. The signal S was observed after all annealing temperatures investigated. The electrical characteristics of this DL match those often ascribed to a higher-order vacancy-related defect complex [24]. In contrast to all other afore-mentioned DLs, DL S was also recorded in non-implanted reference samples, though, only at the highest-available amplification level of the DLTS system. This observation is in opposition to an assignment of DL S to a vacancy-related defect, at least of the complete signal amplitude. Other authors have proposed a nitrogen-related defect as origin for a similar mid-gap level (see, e.g., Refs. [31, 32]).

Figure 3 depicts the concentrations of different DLs in a sample implanted with 2.5-MeV protons (without Al-absorber) in dependence of the proton fluence after annealing at a high thermal budget. The DL concentrations were measured in a volume directly at the irradiated surface of the sample. The data show an approximately linear dependence of the DL concentrations on the proton fluence for most of the DLs. The concentration of the DL G, however, exhibits a decline with increasing fluences above 10^{14} cm^{-2}. This behavior of the DL G somewhat contradicts its previous identification with the V_2O defect, particularly as other allegedly oxygen-related DLs as, e.g., the DL L show an opposite behavior. A similar observation regarding the DL G can be made in the concentration–depth profiles depicted in Fig. 4. In this experiment, the proton fluence was kept constant at 4×10^{14} cm^{-2} and the concentrations of the DLs were extracted in different depths after beveling the implanted and annealed sample. The concentration of the primary damage varies with the depth due to the characteristic stopping power profile of high-energy particles

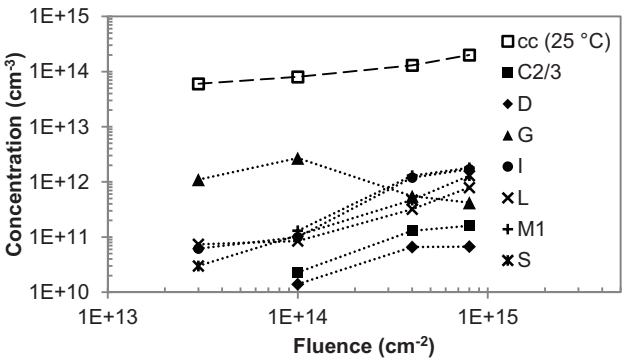

Figure 3 Concentrations of the cc at 25 °C and several DLs in dependence on the fluence of 2.5-MeV protons after annealing at 470 °C for 5 h in the surface volume (~2–15 μm) of the samples.

[1] A detailed report on the topic will be put forward by the authors at the 226th ECS meeting in Cancun, Mexico.

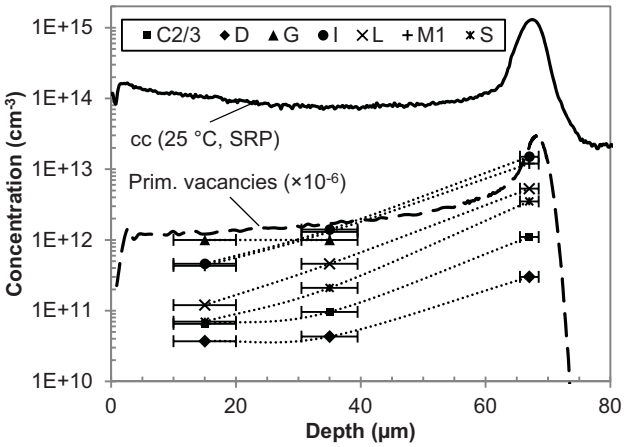

Figure 4 Concentration–depth profiles of the cc at 25 °C and several DLs in a sample implanted with 2.5-MeV protons to a fluence of $4 \times 10^{14}\,cm^{-2}$ after annealing at 470 °C for 5 h. The primary vacancy distribution was simulated by SRIM [33].

(see, e.g., the simulated distribution of the primary vacancies in Fig. 4). Due to their low amplitudes, the signals of the DLs K and P are partially covered by other DLs (see also Fig. 1), so that their concentrations were not considered for extraction from the data at hand. Figure 4 shows, in principle, an increase of the concentrations of all depicted DLs with increasing concentration of the primary vacancies, except for DL G. At a depth beyond 40 μm the DL G was not detected in this sample.

4 Conclusion DLTS-measurements of MeV proton-implanted silicon samples annealed at temperatures typically used for proton-implantation doping have been analyzed. The study reveals a multitude of deep-level defects remaining active even after thermal anneals at temperatures up to 500 °C for 5 h. Even for the high annealing temperatures, defect concentrations up to $10^{13}\,cm^{-3}$ are detected. The temperature range of the induced defects for proton fluences above several $10^{13}\,cm^{-2}$ extends to higher temperatures than usually associated with these defects.

References

[1] V. A. Kozlov and V. V. Kozlovski, Semiconductors **35**, 735 (2001).
[2] R. Job, J. G. Laven, F.-J. Niedernostheide, H.-J. Schulze, H. Schulze, and W. Schustereder, Phys. Status Solidi A **209**, 1940 (2012).
[3] D. C. Sawko and J. Bartko, IEEE Trans. Nucl. Sci. **30**, 1756 (1983).
[4] R. Siemieniec, F.-J. Niedernostheide, H.-J. Schulze, W. Südkamp, U. Kellner-Werdehausen, and J. Lutz, J. Electrochem. Soc. **153**, G108 (2006).
[5] M. W. Hüppi, J. Appl. Phys. **68**, 2702 (1990).
[6] G. H. Schwuttke, K. Brack, E. F. Gorey, A. Kahan, and L. F. Lowe, Radiat. Eff. **6**, 103 (1970).
[7] Y. Zohta, Y. Ohmura, and M. Kanazawa, Jpn. J. Appl. Phys. **10**, 532 (1971).
[8] J. G. Laven, H.-J. Schulze, V. Häublein, F.-J. Niedernostheide, H. Schulze, H. Ryssel, and L. Frey, AIP Conf. Proc. **1321**, 257 (2011).
[9] W. Wondrak and D. Silber, Phys. B **129**, 322 (1985).
[10] P. Voß, Solid-State Electron. **17**, 655 (1974).
[11] M. Nemoto, T. Yoshimura, and H. Nakazawa, Appl. Phys. Express **1**, 051404 (2008).
[12] J. G. Laven, H.-J. Schulze, V. Häublein, F.-J. Niedernostheide, H. Schulze, H. Ryssel, and L. Frey, Phys. Status Solidi C **8**, 697 (2011).
[13] J. G. Laven, R. Job, H.-J. Schulze, F.-J. Niedernostheide, W. Schustereder, and L. Frey, ECS J. Solid State Sci. Technol. **2**, P389 (2013).
[14] V. Komarnitskyy and P. Hazdra, ECS Trans. **25**, 55 (2009).
[15] S. Weiss and R. Kassing, Solid-State Electron. **31**, 1733 (1988).
[16] L. C. Kimerling and J. L. Benton, Appl. Phys. Lett. **39**, 410 (1981).
[17] E. Simoen, C. Claeys, J. M. Rafí, and A. G. Ulyashin, Mater. Sci. Eng. B **134**, 189 (2006).
[18] R. B. Capaz, L. V. C. Assali, L. C. Kimerling, K. Cho, and J. D. Joannopoulos, Phys. Rev. B **59**, 4898 (1999).
[19] P. Hazdra and V. Komarnitskyy, Mater. Sci. Eng. B **159–160**, 346 (2009).
[20] J. Coutinho, R. Jones, P. R. Briddon, S. Öberg, L. I. Murin, V. P. Markevich, and J. L. Lindström, Phys. Rev. B **62**, 014109 (2001).
[21] L. C. Kimerling, J. Appl. Phys. **45**, 1839 (1975).
[22] M.-L. David, E. Oliviero, C. Blanchard, and J. F. Barbot, Nucl. Instr. Meth. Phys. Res. B **186**, 309 (2002).
[23] J. Coutinho, R. Jones, S. Öberg, and P. R. Briddon, Phys. B **340–342**, 523. (2003).
[24] P. Pellegrino, P. Lévêque, J. Lalita, A. Hallén, C. Jagadish, and B. G. Svensson, Phys. Rev. B **64**, 195211 (2001).
[25] G. Alfieri, E. V. Monakhov, B. S. Avset, and B. G. Svensson, Phys. Rev. B **68**, 233202 (2003).
[26] A. O. Evwaraye and E. Sun, J. Appl. Phys. **47**, 3776 (1976).
[27] P. Lévêque, P. Pellegrino, A. Hallén, B. G. Svensson, and V. Privitera, Nucl. Instrum. Methods Phys. Res B **174**, 297 (2001).
[28] J. Coutinho, V. J. B. Torres, R. Jones, S. Öberg, and P. R. Briddon, J. Phys.: Condens. Matter. **15**, S2809 (2003).
[29] B. G. Svensson, A. Hallén, and B. U. R. Sundqvist, Mater. Sci. Eng. B **4**, 285 (1989).
[30] K. B. Nielsen, L. Dobaczewski, K. Goscinski, R. Bendesen, O. Andersen, and B. B. Nielsen, Phys. B **273–274**, 167 (1999).
[31] K. Kakumoto and Y. Takano, *Proc. Int. Symp. on Advanced Science and Technology in Silicon*, p. 437 (1996).
[32] J. P. Goss, I. Hahn, R. Jones, P. R. Briddon, and S. Öberg, Phys. Rev. B **67**, 045206 (2003).
[33] J. F. Ziegler, M. D. Ziegler, and J. P. Biersack, SRIM (1984), http://www.srim.org.

